HHS Public Access

Author manuscript

Emerg Radiol. Author manuscript; available in PMC 2023 September 27.

Published in final edited form as:

Emerg Radiol. 2023 August ; 30(4): 435–441. doi:10.1007/s10140-023-02149-2.

Pulmonary contusion: automated deep learning-based quantitative visualization

Nathan Sarkar[1], **Lei Zhang**[1], **Peter Campbell**[1], **Yuanyuan Liang**[2], **Guang Li**[1], **Mustafa Khedr**[1], **Udit Khetan**[1], **David Dreizin**[1]

[1]Department of Diagnostic Radiology and Nuclear Medicine, R Adams Cowley Shock Trauma Center, University of Maryland School of Medicine, 22 S Greene St, Baltimore, MD 21201, USA

[2]Department of Epidemiology & Public Health, University of Maryland School of Medicine, Baltimore, MD, USA

Abstract

Purpose—Rapid automated CT volumetry of pulmonary contusion may predict progression to Acute Respiratory Distress Syndrome (ARDS) and help guide early clinical management in at-risk trauma patients. This study aims to train and validate state-of-the-art deep learning models to quantify pulmonary contusion as a percentage of total lung volume (Lung Contusion Index, or auto-LCI) and assess the relationship between auto-LCI and relevant clinical outcomes.

Methods—302 adult patients (age ≥ 18) with pulmonary contusion were retrospectively identified from reports between 2016 and 2021. nnU-Net was trained on manual contusion and whole-lung segmentations. Point-of-care candidate variables for multivariate regression included oxygen saturation, heart rate, and systolic blood pressure on admission. Logistic regression was used to assess ARDS risk, and Cox proportional hazards models were used to determine differences in ICU length of stay and mechanical ventilation time.

Results—Mean Volume Similarity Index and mean Dice scores were 0.82 and 0.67. Interclass correlation coefficient and Pearson r between ground-truth and predicted volumes were 0.90 and 0.91. 38 (14%) patients developed ARDS. In bivariate analysis, auto-LCI was associated with ARDS ($p < 0.001$), ICU admission ($p < 0.001$), and need for mechanical ventilation ($p < 0.001$). In multivariate analyses, auto-LCI was associated with ARDS ($p = 0.04$), longer length of stay in the ICU ($p = 0.02$) and longer time on mechanical ventilation ($p = 0.04$). AUC of multivariate regression to predict ARDS using auto-LCI and clinical variables was 0.70 while AUC using auto-LCI alone was 0.68.

Conclusion—Increasing auto-LCI values corresponded with increased risk of ARDS, longer ICU admissions, and longer periods of mechanical ventilation.

Keywords

ARDS; Artificial intelligence; Pulmonary contusion; Quantitative imaging; Segmentation

✉David Dreizin, daviddreizin@gmail.com.

Conflict of interest The authors have no conflicts of interest to declare that are relevant to the content of this article.

Introduction

Pulmonary contusion is a well-described clinical entity seen in acute thoracic trauma in which rapid acceleration-deceleration disrupts pulmonary capillaries, leading to localized edema and extravasation of blood [1, 2]. This manifests on computed tomography (CT) with a characteristic appearance of mixed focal ground-glass and consolidative opacities sparing the subpleural regions [3, 4].

Pulmonary contusion is a risk factor for development of Acute Respiratory Distress Syndrome (ARDS) [5], which has an in-hospital mortality rate of 40% [6, 7] and typically develops at a peak latency of approximately 72 h after injury [2]. Most previous works have assessed pulmonary contusion either as a binary (i.e., presence or absence of contusion) or coarse categorical predictor [8], or by using semi-automated software requiring end-user proficiency with specific platforms and effort which is non-negligible in the time-sensitive trauma setting. One such semi-automated method by Miller et al. found that patients with contusions involving at least 20% of the total lung volume had an 82% risk of developing ARDS [5]. The degree of pulmonary contusion has also been linked to hospital stay, need for ICU admission, and need for mechanical ventilation [9–11]. Automated quantitative visualization of percent lung involvement (i.e., verifiable voxelwise segmentations and measurements of contusion indexed to total lung volumes, which we henceforth refer to as the automated Lung Contusion Index, or auto-LCI), may serve as a precise, objective, and granular predictor of ARDS risk and related adverse outcomes.

Recent end-to-end automated computer vision pipelines have achieved state-of-the-art results for a variety of challenging problems requiring fine-detail segmentation of irregular, ill-defined, multifocal pathologic features with wide ranges of target volumes [12–19]. During the COVID pandemic, a variety of robust multiscale methods have emerged for quantitative visualization of infiltrates on CT, with nnU-Net achieving best-in-class performance for this task in deep learning challenges [20]. Clinical validation of an nnU-Net based approach was recently described in *Radiology* by Lessmann et al. [21].

The purpose of this study is to 1) train and validate a deep learning model to quantify pulmonary contusion as a percentage of total lung volume and 2) assess the relationship between percentage of lung contused and negative clinical outcomes including development of ARDS.

Methods

Dataset

This observational study is part of an exempt-status protocol approved by the University of Maryland, Baltimore Institutional Review Board. Patients were retrospectively identified from an MPower-generated database of 5424 sequential patients treated at the study site (a level I trauma center) who underwent admission trauma CT between Jul 1, 2016, and March 16, 2021. 302 patients with pulmonary contusions were manually identified from radiology CT reports by staff under the supervision of a radiologist attending. Studies were performed on either a 128-section CT scanner (Somatom Force; Siemens, Erlangen Germany), or a

64-section CT scanner (Brilliance; Philips Healthcare, Andover, Mass.) and were archived as 3-mm thickness images. All images of the chest were acquired at our institution in the arterial phase. Pulmonary contusions in all 302 patients were then manually segmented from Neuroimaging Informatics Technology Initiative (NifTI) CT images by trained members of the research team using 3D Slicer [22], with each study edited by a senior trauma radiologist with 10 years of experience in voxelwise labeling.

Clinical data were obtained from chart review of the medical record. Datapoints obtained included: sex, age, Abbreviated Injury Scale (AIS) [23] and Injury Severity Score (ISS) [24], admission vital signs, whether the patient was admitted to the ICU, whether mechanical ventilation was required, days spent in the ICU, days spent on mechanical ventilation, total days spent in the hospital, whether the patient developed ARDS during their hospitalization, and whether the patient expired. ARDS status was determined by a documented diagnosis of ARDS in a provider note, following Berlin criteria [25].

Exclusion criteria were i) Catastrophic head injury determined by Head/Brain AIS score of 6, ii) lack of or ambiguous ARDS data that did not meet Berlin criteria, and iii) missing clinical values. 22 patients were excluded, resulting in a total of 280 patients for clinical analysis. Of these patients, 223 (79%) were male, median age was 37 years (IQR 22–49), and 38 patients (14%) developed ARDS during their hospitalization. Further patient characteristics are shown in Table 1.

Deep learning method

nnU-Net [26] was chosen as the framework to automate segmentation. In COVID-19 patients, nnU-Net has shown success in quantifying lung infiltrates [21], a radiographic finding that has similarities to the CT appearance of pulmonary contusion, with multifocal ground-glass and consolidative opacities of highly variable volume. nnU-Net is a state-of-the-art deep learning framework that replaces user-dependent hyperparameter optimization with a data-driven strategy of hyperparameter selection, stipulating that poorly chosen hyperparameters often have a greater effect on the performance of the network than the network architecture itself [26, 27]. Briefly, the framework trains 4 models: a 2D U-Net, a low-resolution 3D U-Net, a full-resolution 3D U-Net, and a full-resolution cascaded 3D U-Net. It also creates an ensemble model aggregating these methods. All image preprocessing and training parameters are automatically chosen by the framework using a rules-based algorithm to create a “pipeline fingerprint” which is unique to a given dataset. This approach resulted in state-of-the-art performance on 33 of 53 public segmenting challenges, highlighting the robustness of the method. All neural networks were validated in fivefold cross-validation. Model performance was evaluated with overlap and volume-based metrics including a Dice similarity coefficient (DSC), volume similarity index (VS), Pearson’s r, and Interclass correlation coefficient (ICC).

For segmenting total lung volume, a public dataset of 402 patients from the NSCLC-Radiomics Cancer Imaging Archive dataset was used to train an additional nnU-Net model [28]. fivefold cross-validation was performed on the ground-truth labels from that archive. The model was then applied in inference to our CT dataset to determine total lung volume.

Statistical analysis

Development of ARDS was used as the primary outcome. Secondary outcomes included need for ICU admission, need for mechanical ventilation, time spent in the ICU, time spent on mechanical ventilation, and total hospital length of stay.

Mann Whitney U test and Chi square test were performed to test association between each of the clinically identified variable (age, sex, ISS, etc.) and relevant outcomes. Mann–Whitney U was used for all continuous variables as all were non-normal, and Chi square was used for all categorical variables. Logistic regression was performed to predict ARDS risk using auto-LCI and other clinical variables that were significant ($p < 0.05$) in bivariate analysis and available at point-of-care. This logistic regression model was used to create an approximate ARDS risk stratification based on various levels of auto-LCI while other predictors were held at their mean values.

For secondary outcome analysis with time-to-event data pertaining to length of stay and extubation, patients who expired ($N = 5$) were excluded. Cox proportional hazards regression was performed using the auto-LCI and point-of-care variables as in the primary analysis to predict 1) time to discharge from the ICU (among patients admitted to the ICU, $N = 76$) and 2) time until extubation (among patients who were mechanically ventilated, $N = 95$). All statistical analyses were performed with STATA 17 statistical software.

Results

Deep learning results

Median auto-LCI was 3.03 (IQR: 0.84 – 8.52) for the total population. Group differences are shown in Table 1. Mean Dice and Volume Similarity Index (VSI) scores of the 2D, 3D low-resolution, 3D full-resolution, 3D cascaded full-resolution, and ensemble models are shown in Table 2. As the ensemble model showed the best performance, it was used for all further analysis. Mean Dice and VSI scores of the ensemble model were 0.67 (SD: 0.20) and 0.82 (SD: 0.20). Interclass correlation coefficient (ICC) between ground-truth contusion volume and automated contusion volume was 0.90 (95% CI: 0.87 to 0.92), Pearson's r was 0.91 (95% CI: 0.89 to 0.93), and Bland–Altman mean bias analysis demonstrated a mean undermeasurement of the automated contusion volumes by 13.5 mL with a range of automated volumes of 0 mL to 1378 mL. Pearson's r values ≥ 0.80 are indicative of strong correlation and ICC values ≥ 0.75 are considered to indicate excellent agreement [29]. Whole-lung segmentation resulted in a mean Dice score of 0.94 in the NSCLC dataset. Representative images of segmentation are shown in Fig. 1.

Clinical outcomes

In bivariate analyses (Table 1), auto-LCI was strongly associated with ARDS (7.90% (IQR: 3.00–15.10)- ARDS subgroup vs 2.50% (IQR: 0.63–7.10)- subgroup without ARDS, $p < 0.001$) (Fig. 2). Auto-LCI was also associated with ICU admission and need for mechanical ventilation as binary outcomes ($p < 0.001$). Variables significantly correlated with the primary outcome of ARDS development included admission systolic blood pressure (ARDS 128 mmHg (IQR 112–142) vs Non-ARDS 140 mmHg (IQR 127–156), $p = 0.02$),

O_2 saturation (ARDS 95.5% (IQR: 88.8–98.0) vs No ARDS 98% (95.0–100), $p = 0.01$), admission to the ICU (ARDS 37/38 (97%) vs Non-ARDS 39/242 (16%), $p < 0.001$), and the injury severity score (ISS) (ARDS 29 (IQR: 22–34)) vs Non-ARDS 14 (IQR: 10–22), $p < 0.001$).

Candidate variables included in multivariate analyses of the primary and secondary outcomes were auto-LCI, systolic blood pressure, and O_2 saturation. Systolic blood pressure and O_2 saturation were chosen because among the variables significantly associated with ARDS risk in bivariate analysis (Table 1), these two are available at time of presentation. This contrasts with ICU admission status (a future event) or ISS (a score derived by trauma registry coders post-hoc).

A logistic regression model using the above three variables to predict ARDS status showed that auto-LCI (Unit-odds ratio 1.041 [95% CI: 1.001–1.082], $p = 0.04$) and O_2 Saturation (Unit-odds Ratio 0.906 [95% CI: 0.835–0.983], $p = 0.02$) were statistically significant predictors of ARDS. A Hosmer–Lemeshow goodness-of-fit test showed that this model was well-fitted to the data ($p = 0.74$). The auto-LCI unit-odds ratio can be interpreted as a 1-percentage point increase in auto-LCI corresponding with a 4.1% increase in the odds of ARDS. 10, 20, 30, 40, 50, and 60-percentage point increases in auto-LCI increase the odds of ARDS by 49%, 123%, 233%, 398%, 644%, and 1012% respectively. The AUC of this logistic model to predict ARDS was 0.70 (95% CI: 0.61–0.80). AUC of auto-LCI alone to predict ARDS was 0.68 (95% CI: 0.58–0.77) whereas the AUCs of O_2 saturation and systolic blood pressure to predict ARDS were 0.63 (95% CI: 0.52–0.74) and 0.62 (95% CI: 0.51–0.73), respectively.

Multivariate Cox proportional hazards regression showed that among patients admitted to the ICU who did not expire, auto-LCI was significantly associated with increased ICU Length of Stay (Unit-hazard Ratio 0.977 [95% CI: 0.957–0.997], $p = 0.02$). Among patients who were mechanically ventilated and did not expire, auto-LCI was also associated with longer time on mechanical ventilation (Unit-hazard Ratio 0.977 [95% CI: 0.956–0.999], $p = 0.04$). In contrast to survival analysis in which hazard ratio < 1 indicates prolonged survival (positive outcome), in this analysis hazard ratio < 1 indicates prolonged ICU stay or mechanical ventilation (negative outcomes).

Discussion

Traumatic injury to the chest is associated with high morbidity and mortality [30–32]. A common [33–35] proximate cause of disability from traumatic chest injury is the progression to ARDS within a few days. Pulmonary contusions are frequently identified on the admission chest CT in traumatic chest injuries and are known to be an independent risk factor for development of ARDS [5]. When ARDS is identified and treated earlier, patients appear to have improved outcomes [36, 37]. Thus, quantitation of pulmonary contusion volume from a patient's admission chest CT as a function of total lung volume (the auto-LCI) represents a precise metric that is potentially exploitable early in the treatment course of chest trauma to determine risk of development of ARDS and other serious complications, which could result in improved clinical outcomes.

Precision medicine-oriented automated quantitative visualization tools are in development for a variety of use cases in emergency and trauma radiology and are considered desirable by practitioners in the field [38, 39]. The primary barrier to pulmonary contusion volume quantification has been the need to automatically segment contusion. Since pulmonary contusion exists on multiple spatial scales (lobar vs focal) and does not have a consistent density, hand-crafted feature engineering-based segmentation methods are not well-suited to the task of pulmonary contusion segmentation. Deep learning methods have been shown to overcome many of these challenges [40]. Prior reports of deep learning methods to segment pulmonary contusion volumetrically did not evaluate ARDS [11]. Radiomics-based methods have been employed for ARDS prediction but did not consider the overall injury burden as expressed by volume or percent of the lungs involved, with interpretable and easily verifiable segmentation masks or contours [41]. We were able to match a precise volumetric index to clinical data to achieve a holistic analysis encompassing the course of hospitalization.

In our dataset of 302 patients, nnU-Net segmented pulmonary contusion volumes with high precision and accuracy at a level comparable with that achieved for a similarly complex task involving irregular, ill-defined, and multifocal targets with highly variable appearances and volumes in a public COVID Lung CT lesion segmentation challenge [42]. ICC and Pearson's r values indicate excellent agreement between manual ground-truth and automated segmentations.

The automated output, given as the percentage of the total lung volume contused (auto-LCI), was significantly associated with increased risk for ARDS in bivariate analysis and was found to be an independent predictor in a multivariate model. This indicates that the auto-LCI provides additional information useful for predicting a patient's ARDS risk when accounting for clinical predictors available at the initial point of care, namely systolic blood pressure and O_2 saturation. Auto-LCI was also found to provide information useful for predicting negative outcomes, specifically, prolonged length of stay in the ICU and a prolonged time on mechanical ventilation. Proprietary and containerized open-source software is available that converts NifTI to DICOM for visualization of segmentations in the reading room along with quantitative results as DICOM structured report elements [43].

Ultimately, we envision that these findings will provide part of the foundation for a personalized decision support pipeline that incorporates pulmonary contusion detection, segmentation, and ARDS risk-stratification for use immediately at the time of initial chest CT. CT chest is nearly ubiquitous in serious chest trauma in the US [44], and such a method would be expected to have broad applicability.

There are several limitations to our work, namely a single-institution dataset that was collected retrospectively. Therefore prior to clinical use, our method needs to be validated or further calibrated in a prospective multicenter study with heterogeneous data sources to ensure generalizability. Additionally, there may be information captured by ISS and AIS that is not accounted for in our multivariate model. Future models may include other elements of injury severity such as flail chest, number of rib fractures, and hemothorax. Volumetric

measurement of body composition parameters may further improve outcome prediction in trauma [45].

In conclusion, our automated lung contusion index, derived using nnU-Net, a state-of-the-art segmentation method, was significantly associated with development of ARDS and relevant clinical outcomes. Future multicenter and prospective work will focus on generalizability.

Acknowledgements

NIH K08 EB027141-01A1 (PI: David Dreizin, MD)

Data availability

Data supporting the findings of this study are available upon request to the corresponding author.

References

1. Ahmad Ganie F, Lone H, Nabi Lone G, Lateef Wani M, Singh S, Majeed Dar A et al. (2023) Lung contusion: a clinico-pathological entity with unpredictable clinical course. Bull Emerg Trauma 1:7–16
2. Cohn SM, DuBose JJ (2010) Pulmonary contusion: an update on recent advances in clinical management. World J Surg 34(8):1959–1970. 10.1007/S00268-010-0599-9 [PubMed: 20407767]
3. Chong WH, Saha BK, Austin A, Chopra A (2021) The significance of subpleural sparing in ct chest: a state-of-the-art review. Am J Med Sci 361:427–435. 10.1016/J.AMJMS.2021.01.008 [PubMed: 33487401]
4. Donnelly LF, Klosterman LA (1997) Subpleural sparing: a CT finding of lung contusion in children. Radiology 204:385–387. 10.1148/RADIOLOGY.204.2.9240524 [PubMed: 9240524]
5. Miller PR, Croce MA, Bee TK, Qaisi WG, Smith CP, Collins GL et al. (2001) ARDS after pulmonary contusion: accurate measurement of contusion volume identifies high-risk patients. J Trauma 51:223–230. 10.1097/00005373-200108000-00003 [PubMed: 11493778]
6. Bellani G, Laffey JG, Pham T, Fan E, Brochard L, Esteban A et al. (2016) Epidemiology, patterns of care, and mortality for patients with acute respiratory distress syndrome in intensive care units in 50 countries. JAMA 315:788–800. 10.1001/JAMA.2016.0291 [PubMed: 26903337]
7. Villar J, Blanco J, Añón JM, Santos-Bouza A, Blanch L, Ambrós A et al. (2011) The ALIEN study: incidence and outcome of acute respiratory distress syndrome in the era of lung protective ventilation. Intensive Care Med 37:1932–1941. 10.1007/S00134-011-2380-4 [PubMed: 21997128]
8. Sayed MS, Elmeslmany KA, Elsawy AS, Mohamed NA (2022) The validity of quantifying pulmonary contusion extent by lung ultrasound score for predicting ARDS in blunt thoracic trauma. Crit Care Res Pract 2022:1. 10.1155/2022/3124966
9. Zingg SW, Millar DA, Goodman MD, Pritts TA, Janowak CF (2021) The association between pulmonary contusion severity and respiratory failure. Respir Care 66:1665–1672. 10.4187/RESPCARE.09145 [PubMed: 34584011]
10. Choi J, Tennakoon L, You JG, Kaghazchi A, Forrester JD, Spain DA (2021) Pulmonary contusions in patients with rib fractures: The need to better classify a common injury. Am J Surg 221:211–215. 10.1016/j.amjsurg.2020.07.022 [PubMed: 32854902]
11. Choi J, Mavrommati K, Li NY, Patil A, Chen K, Hindin DI et al. (2022) Scalable deep learning algorithm to compute percent pulmonary contusion among patients with rib fractures. J Trauma Acute Care Surg 93:461. 10.1097/TA.0000000000003619 [PubMed: 35319542]
12. Dreizin D, Zhou Y, Zhang Y, Tirada N, Yuille AL (2020) Performance of a deep learning algorithm for automated segmentation and quantification of traumatic pelvic hematomas on CT. J Digit Imaging 33:243–251. 10.1007/S10278-019-00207-1 [PubMed: 31172331]

13. Zhou Y, Dreizin D, Wang Y, Liu F, Shen W, Yuille AL (2022) External attention assisted multi-phase splenic vascular injury segmentation with limited data. IEEE Trans Med Imaging 41:1346–1357. 10.1109/TMI.2021.3139637 [PubMed: 34968179]

14. Dreizin D, Zhou Y, Chen T, Li G, Yuille AL, McLenithan A et al. (2020) Deep learning-based quantitative visualization and measurement of extraperitoneal hematoma volumes in patients with pelvic fractures: Potential role in personalized forecasting and decision support. J Trauma Acute Care Surg 88:425–433. 10.1097/TA.0000000000002566 [PubMed: 32107356]

15. Dreizin D, Zhou Y, Fu S, Wang Y, Li G, Champ K et al. (2020) a multiscale deep learning method for quantitative visualization of traumatic hemoperitoneum at CT: assessment of feasibility and comparison with subjective categorical estimation. Radiol Artif Intell 2:1–9. 10.1148/RYAI.2020190220

16. Dreizin D, Chen T, Liang Y, Zhou Y, Paes F, Wang Y et al. (2021) Added value of deep learning-based liver parenchymal CT volumetry for predicting major arterial injury after blunt hepatic trauma: a decision tree analysis. Abdom Radiol (NY) 46:2556–2566. 10.1007/S00261-020-02892-X [PubMed: 33469691]

17. Chen H, Unberath M, Dreizin D (2023) Toward automated interpretable AAST grading for blunt splenic injury. Emerg Radiol 30:41–50. 10.1007/S10140-022-02099-1 [PubMed: 36371579]

18. Dreizin D, Nixon B, Hu J, Albert B, Yan C, Yang G et al. (2022) A pilot study of deep learning-based CT volumetry for traumatic hemothorax. Emerg Radiol 29:995. 10.1007/S10140-022-02087-5 [PubMed: 35971025]

19. Zhou Y, Dreizin D, Li Y, Zhang Z, Wang Y, Yuille A (2019) Multi-scale attentional network for multi-focal segmentation of active bleed after pelvic fractures. Lecture Notes Comput Sci (Including Subseries Lecture Notes in Artif Intell Lecture Notes Bioinformatics) 11861 LNCS:461–9. 10.1007/978-3-030-32692-0_53/COVER

20. Roth HR, Xu Z, Tor-Díez C, Sanchez Jacob R, Zember J, Molto J et al. (2022) Rapid artificial intelligence solutions in a pandemic—The COVID-19–20 Lung CT Lesion Segmentation Challenge. Med Image Anal 82:102605. 10.1016/j.media.2022.102605 [PubMed: 36156419]

21. Lessmann N, Sánchez CI, Beenen L, Boulogne LH, Brink M, Calli E et al. (2021) Automated assessment of COVID-19 reporting and data system and chest CT severity scores in patients suspected of having COVID-19 using artificial intelligence. Radiology 298:E18–28. 10.1148/RADIOL.2020202439/ASSET/IMAGES/LARGE/RADIOL.2020202439.FIG6.JPEG [PubMed: 32729810]

22. Fedorov A, Beichel R, Kalpathy-Cramer J, Finet J, Fillion-Robin JC, Pujol S et al. (2012) 3D Slicer as an image computing platform for the Quantitative Imaging Network. Magn Reson Imaging 30:1323–1341. 10.1016/j.mri.2012.05.001 [PubMed: 22770690]

23. Loftis KL, Price J, Gillich PJ (2018) Evolution of the Abbreviated Injury Scale: 1990–2015. Traffic Inj Prev 19:S109–S113. 10.1080/15389588.2018.1512747 [PubMed: 30543458]

24. Baker SP, O'Neill B, Haddon W, Long WB (1974) The injury severity score: a method for describing patients with multiple injuries and evaluating emergency care. J Trauma 14:187–196. 10.1097/00005373-197403000-00001 [PubMed: 4814394]

25. Ferguson ND, Fan E, Camporota L, Antonelli M, Anzueto A, Beale R et al. (2012) The Berlin definition of ARDS: an expanded rationale, justification, and supplementary material. Intensive Care Med 38:1573–1582. 10.1007/S00134-012-2682-1 [PubMed: 22926653]

26. Isensee F, Jaeger PF, Kohl SAA, Petersen J, Maier-Hein KH (2020) nnU-Net: a self-configuring method for deep learning-based biomedical image segmentation. Nat Methods 18(2):203–11. 10.1038/s41592-020-01008-z [PubMed: 33288961]

27. Litjens G, Kooi T, Bejnordi BE, Setio AAA, Ciompi F, Ghafoorian M et al. (2017) A survey on deep learning in medical image analysis. Med Image Anal 42:60–88. 10.1016/J.MEDIA.2017.07.005 [PubMed: 28778026]

28. Aerts HJWL, Velazquez ER, Leijenaar RTH, Parmar C, Grossmann P, Cavalho S et al. (2014) Decoding tumour phenotype by noninvasive imaging using a quantitative radiomics approach. Nat Commun 5:1–9. 10.1038/ncomms5006

29. Zou KH, Tuncali K, Silverman SG (2003) Correlation and simple linear regression. Radiology 227:617–622. 10.1148/RADIOL.2273011499 [PubMed: 12773666]

30. Dreizin D, Munera F (2012) Blunt polytrauma: evaluation with 64-section whole-body CT angiography. Radiographics 32:609–632. 10.1148/RG.323115099 [PubMed: 22582350]

31. Sangster GP, González-Beicos A, Carbo AI, Heldmann MG, Ibrahim H, Carrascosa P et al. (2007) Blunt traumatic injuries of the lung parenchyma, pleura, thoracic wall, and intrathoracic airways: multidetector computer tomography imaging findings. Emerg Radiol 14:297–310. 10.1007/S10140-007-0651-8 [PubMed: 17623115]

32. Clark GC, Schecter WP, Trunkey DD (1988) Variables affecting outcome in blunt chest trauma: flail chest vs. pulmonary contusion. J Trauma 28:298–304. 10.1097/00005373-198803000-00004 [PubMed: 3351988]

33. Navarrete-Navarro P, Rodriguez A, Reynolds N, West R, Habashi N, Rivera R et al. (2001) Acute respiratory distress syndrome among trauma patients: trends in ICU mortality, risk factors, complications and resource utilization. Intensive Care Med 27:1133–1140. 10.1007/S001340100955 [PubMed: 11534560]

34. Hudson LD, Milberg JA, Anardi D, Maunder RJ (1995) Clinical risks for development of the acute respiratory distress syndrome. Am J Respir Crit Care Med 151:293–301. 10.1164/AJRCCM.151.2.7842182 [PubMed: 7842182]

35. Hoyt DB, Simons RK, Winchell RJ, Cushman J, Hollingsworth-Fridlund P, Holbrook T et al. (1993) A risk analysis of pulmonary complications following major trauma. J Trauma 35:524–531. 10.1097/00005373-199310000-00005 [PubMed: 8411274]

36. Bellani G, Pham T, Laffey JG (2020) Missed or delayed diagnosis of ARDS: a common and serious problem. Intensive Care Med 46:1180–1183. 10.1007/S00134-020-06035-0/FIGURES/1 [PubMed: 32328723]

37. Yadav H, Thompson BT, Gajic O (2017) Is acute respiratory distress syndrome a preventable disease? Am J Respir Crit Care Med 195:725–736. 10.1164/RCCM.201609-1767CI/SUPPL_FILE/DISCLOSURES.PDF [PubMed: 28040987]

38. Dreizin D, Staziaki PV, Khatri GD, Beckmann NM, Feng Z, Liang Y et al. (2023) Artificial intelligence CAD tools in trauma imaging: a scoping review from the American Society of Emergency Radiology (ASER) AI/ML Expert Panel. Emerg Radiol 30:251. 10.1007/S10140-023-02120-1 [PubMed: 36917287]

39. Agrawal A, Khatri GD, Khurana B, Sodickson AD, Liang Y, Dreizin D (2023) A survey of ASER members on artificial intelligence in emergency radiology: trends, perceptions, and expectations. Emerg Radiol 30:267. 10.1007/S10140-023-02121-0 [PubMed: 36913061]

40. Guo Y, Liu Y, Georgiou T, Lew MS (2018) A review of semantic segmentation using deep neural networks. Int J Multimed Inf Retr 7:87–93. 10.1007/S13735-017-0141-Z/FIGURES/3

41. Röhrich S, Hofmanninger J, Negrin L, Langs G, Prosch H (2021) Radiomics score predicts acute respiratory distress syndrome based on the initial CT scan after trauma. Eur Radiol 31:5443–5453. 10.1007/S00330-020-07635-6/TABLES/5 [PubMed: 33733689]

42. Roth HR, Xu Z, Diez CT, Jacob RS, Zember J, Molto J, et al. (2021) Rapid artificial intelligence solutions in a pandemic - the Covid-19–20 lung CT lesion segmentation challenge. Res Sq. 10.21203/RS.3.RS-571332/V1

43. Zhang L, LaBelle W, Unberath M, Chen H, Hu J, Li G, et al. (2023) A vendor-agnostic, PACS integrated, and DICOM-compatible software-server pipeline for testing segmentation algorithms within the clinical radiology workflow. Res Sq. 10.21203/RS.3.RS-2837634/V1

44. Oikonomou A, Prassopoulos P (2011) CT imaging of blunt chest trauma. Insights Imaging 2:281. 10.1007/S13244-011-0072-9 [PubMed: 22347953]

45. Dreizin D, Rosales R, Li G, Syed H, Chen R (2021) Volumetric markers of body composition may improve personalized prediction of major arterial bleeding after pelvic fracture: a secondary analysis of the Baltimore CT prediction model cohort. Can Assoc Radiol J 72:854–861. 10.1177/0846537120952508 [PubMed: 32910695]

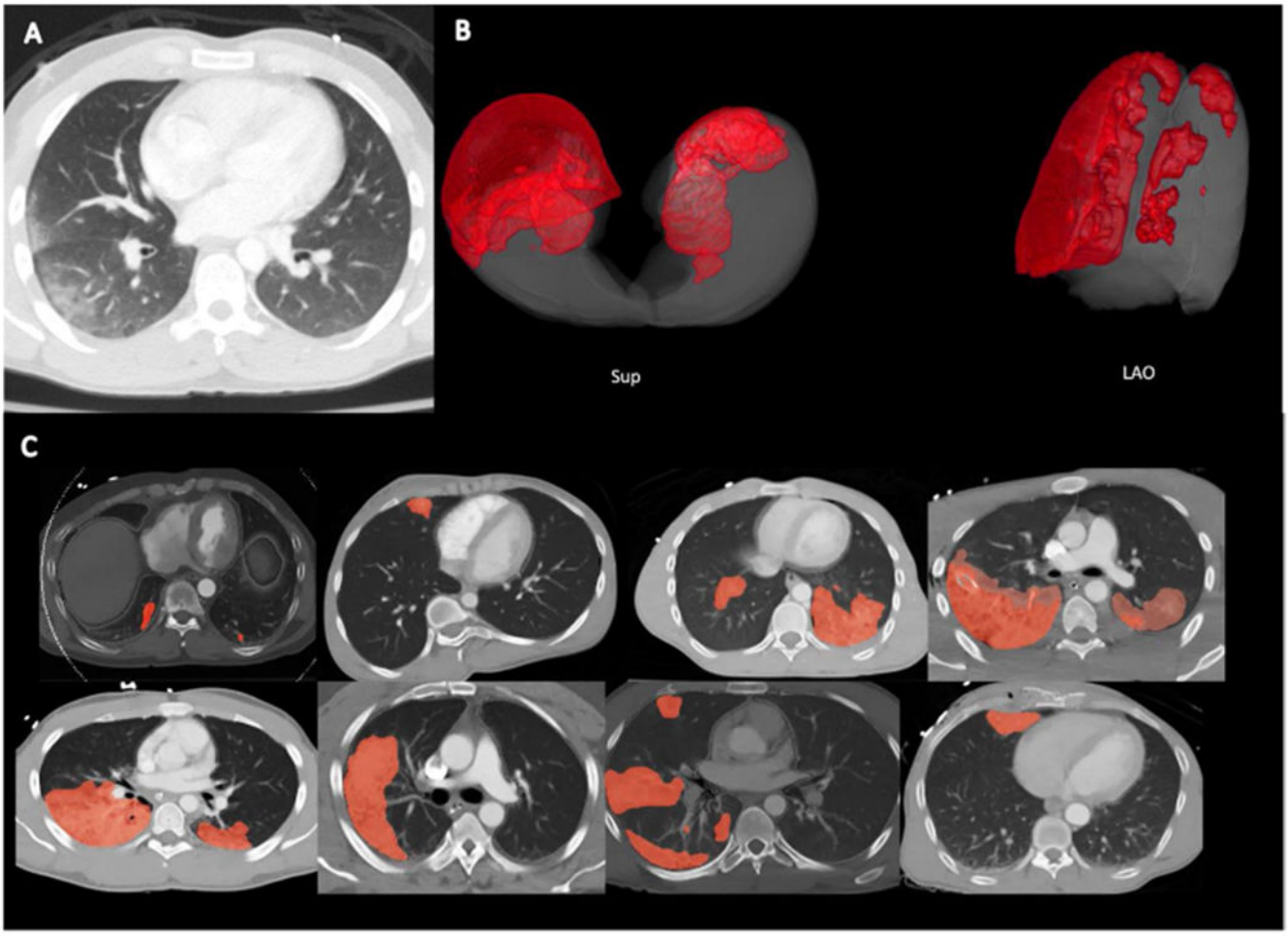

Fig. 1.

A Typical appearance of pulmonary contusion in the right peripheral lung; ground-glass appearance with subpleural sparing. **B** 3D reconstructed images of pulmonary contusion and lung volume. Sup = superior view; LAO = left anterior oblique view. **C** Automated segmentation in 8 representative patients. Light red areas are areas of automated segmentation only. Darker red areas are areas of overlap between manual and automated segmentation. Lung volume is denoted with gray outline, corresponding with the pleural margin in all patients illustrated

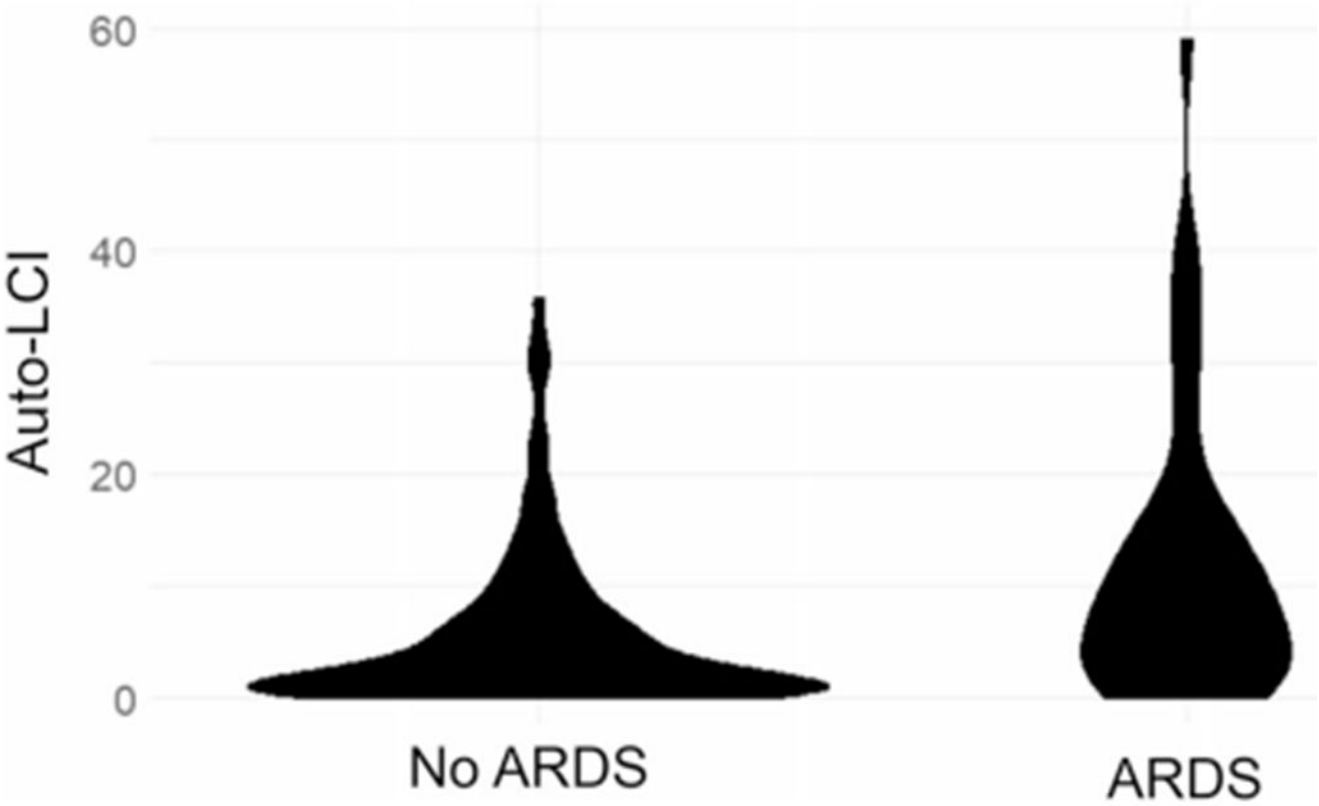

Fig. 2.
Violin plot of the distribution of auto-LCI in non-ARDS patients (left) and ARDS patients (right)

Table 1

Overall and ARDS-stratified patient characteristics

Variable	Total (*N* = 280)	ARDS Status		*p*-value*
		No ARDS (*N* = 242)	ARDS (*N* = 38)	
Sex (Male)	222 (79)	192 (79)	30 (79)	0.96
Age (years)	31 (22–49)	31 (22–29)	29.5 (23–50)	0.75
Systolic Blood Pressure (mmHg)	139 (125–155)	140 (127–156)	128 (112–142)	0.02
Heart Rate (bpm)	91 (80–104)	91 (79–103)	91.5 (82–116)	0.44
O_2 Saturation (%)	97.5 (94–99)	98 (95–100)	95.5 (88.8–98)	0.01
ISS	17 (12–26)	14 (10–22)	29 (22–34)	< 0.001
Expired	5 (2)	3 (1)	2 (5)	0.08
Hospital LOS (days)	3 (1–8)	2 (1–7)	17 (10–33)	< 0.001
Admitted to ICU	76 (27)	39 (16)	37 (97)	< 0.001
ICU LOS (days)	7 (4–18)	6 (3–15)	13 (5–23)	< 0.001
Mechanically Ventilated	95 (34)	58 (24)	37 (97)	< 0.001
Time on Ventilation (days)	3 (2–12)	3 (1–5)	9 (3–19)	< 0.001
Contusion volume (mL)	85 (24–229)	73 (22–199)	200 (86–407)	< 0.001
Total lung volume (mL)	2825 (2259–3496)	2823 (2260–3482)	2852 (2220–3613)	0.73
Auto-LCI (%)	3.03 (0.84–8.52)	2.50 (0.63–7.10)	7.90 (3.00–15.10)	< 0.001

Data are median (IQR) for continuous variables and count (percentage) for binary variables. Vital signs are those first measured on admission; *ISS* Injury Severity Score, *AIS* Abbreviated Injury Scale, *ARDS* Acute Respiratory Distress Syndrome, *LOS* = Length of Stay, *Auto-LCI* Auto-Lung Contusion Index,

** p*-value determined by Mann–Whitney U-test for continuous variables and Chi-squared test for categorical variables

Table 2

Mean Dice Score Coefficient (DSC) and Volume Similarity Index (VSI) of the nnU-Net models

Model	Mean DSC (± SD)	Mean VSI (± SD)
2D	0.60 (± 0.22)	0.77 (± 0.22)
3D low-Resolution	0.65 (± 0.21)	0.80 (± 0.21)
3D full-resolution	0.65 (± 0.20)	0.80 (± 0.20)
3D cascaded full-resolution	0.62 (± 0.21)	0.77 (± 0.23)
Ensemble	0.67 (± 0.20)	0.82 (± 0.20)